Estuarine, Coastal and Shelf Science (1995) **40,** 545–558

Entrainment of Nitrate in the Fraser River Estuary and its Biological Implications. III. Effects of Winds

Kedong Yin[a], Paul J. Harrison[a], Stephen Pond[a] and Richard J. Beamish[b]

[a]*Department of Oceanography, University of British Columbia, Vancouver, British Columbia, V6T 1Z4 Canada and* [b]*Pacific Biological Station, Department of Fisheries and Oceans, Nanaimo, British Columbia, V9R 5K6 Canada*

Received 2 December 1992 and in revised form 14 April 1994

Keywords: nitrate entrainment; nitrate minimum; winds; riverine plume; estuarine plume; mixing; Fraser River; Strait of Georgia

Two 24-h time series of vertical profiles of velocity, salinity, temperature, fluorescence and NO_3 were conducted during weak and strong winds (2·2 and 7·3 m s^{-1}, respectively) to demonstrate wind effects on entrainment of NO_3 near the mouth of the Fraser River. The results showed that wind-induced entrainment of NO_3 was mainly responsible for the increased NO_3 concentrations in the upper layer because shear velocities between the upper and lower layers were great enough to break down the pycnocline and allow diapycnal mixing to occur. Strong shear was indicated by Richardson numbers less than 0·25 near the depth at which flows in the upper and lower layers moved opposite to each other. As a result of wind-induced entrainment and mixing, the NO_3 minimum in the water column was gradually eroded and disappeared at the end of the time series during the strong wind event. The amount of entrained NO_3 under windy conditions (44 mmol m^{-2}) was almost three times that (16 mmol m^{-2}) under weak winds. The high ratios of the amount of entrained NO_3 to river-borne NO_3 (12 under windy conditions and 5·6 under weak winds) indicates that wind-induced entrainment of NO_3 in summer is particularly important for new production. Because turbulent energy came from winds, mixing started at the surface and moved downward. Thus, phytoplankton cells remained in the surface mixed layer, and responded to the entrained nutrients and grew rapidly. Phytoplankton biomass and primary production in the water column increased at the end of the time series, compared to the beginning.

Introduction

Winds act on the surface of a water column and cause vertical mixing, resulting in deepening of the mixed upper layer in the water column (Farmer, 1972; Denman & Powell, 1984; Mann & Lazier, 1991). Nutrient distribution can be controlled by wind mixing (Foster *et al.*, 1985). Winds, along with tides and river discharge, determine the

0272–7714/95/050545+14 $08.00/0

stratification and mixing of the water column in the Strait of Georgia estuary (LeBlond, 1983). The plume characteristics (surface average salinity, horizontal maximum salinity gradient) on the southern section was found to be correlated with the along-strait component of the wind (Royer & Emery, 1982).

The previous studies have shown that entrainment of NO_3 in the Fraser River estuary and in the area beyond the river mouth (a few kilometres away) was influenced by tides and the magnitude of the river discharge: a spring tide and higher river discharge result in more NO_3 entrainment than a neap tide and lower river discharge (Yin *et al.*, 1995*a*,*b*). The river outflow is stronger at lower low water (LLW) during a spring tide than during a neap tide, or during higher river discharge. Thus the velocity shear between the outflow and the layer below is greater during the spring tide or higher river discharge. The stronger shear results in more entrainment. It is expected that shears between the surface layer (the riverine plume or the estuarine plume) and the water below would be increased when sufficiently strong winds blow over it. If the surface layer velocity is great enough under strong winds, shear between the two layers will be sufficient to overcome the stratification and mixing across the pycnocline will take place.

In this study, a wind event during a time series at the same anchored station (station 2, as in Yin *et al.*, 1995*b*) is reported and the mixing effects on the water column and subsequent NO_3 entrainment are described.

Materials and methods

Two time series on 23–24 August 1990 and 7–8 August 1991 at station 2 were conducted to examine effects of winds on entrainment of NO_3. Station 2 is 8 km seaward of the Fraser River mouth in the direction of the axis of the river channel (see Figure 4 in Yin *et al.*, 1995*a*). A continuous vertical profile of salinity, temperature, fluorescence, velocity and nutrients was taken every 3–4 h over a 24-h period when the ship was anchored. An InterOcean S4 was used to measure depth, salinity, temperature and current velocity. A hose was attached to it and seawater pumped into the laboratory on deck while the S4 was slowly lowered. Seawater was continuously pumped from the hose to an AutoAnalyzer for simultaneous analyses of nitrate, silicate, ammonium and phosphate. The details of the vertical profiling and sampling methods are described by Jones *et al.* (1991). The data were smoothed over a 0·5-min time interval to reduce noise due to the ship's motion. The wind speeds were supplied by Atmospheric Environmental Service, Environment Canada. They were recorded at Vancouver International Airport (close to the river mouth) for the time series of 23–24 August 1990 and at Sand Heads (right at the river mouth) for 7–8 August 1991. The tidal height was observed at Point Atkinson and obtained from the Institute of Ocean Science, Department of Fisheries & Oceans, Canada. The river discharge data were recorded at Hope by Water Survey, Environment Canada.

Temperature–salinity (T-S) diagrams were used to calculate the relative proportion, equivalent thickness of the three water types: freshwater, the estuarine plume and the deep seawater, the amount of entrained NO_3 and the estuarine plume contributed fluorescence. The detailed calculation procedure is described in Yin *et al.* (1995*a*).

A gradient Richardson number is often used to indicate the strength of current shear over the stability of a density gradient. The gradient Richardson number was calculated according to the following equation:

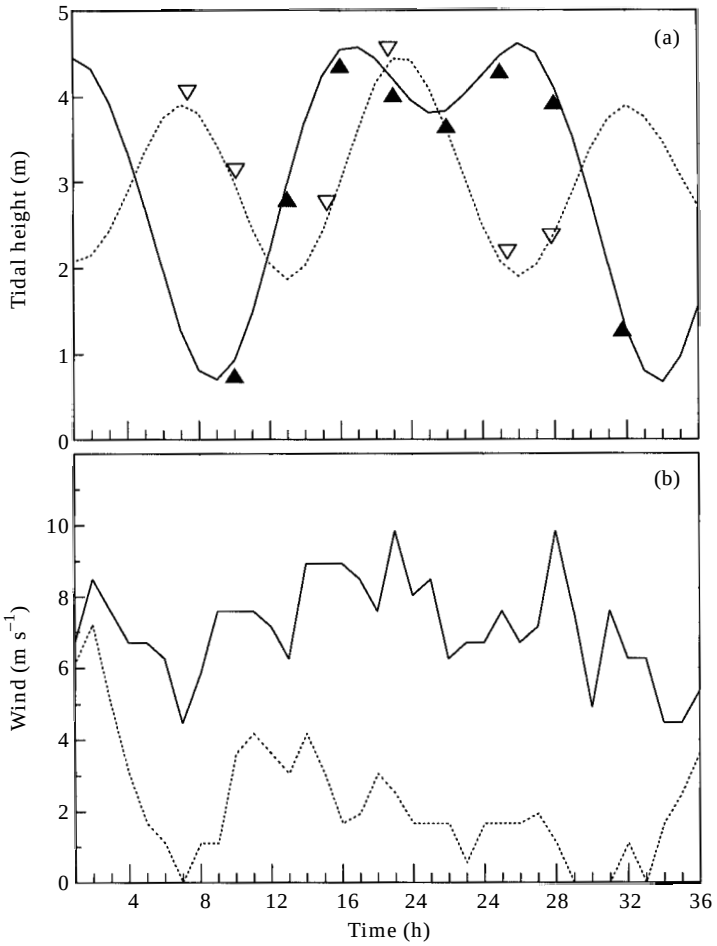

Figure 1. (a) Tidal height and (b) wind speed for the two time series at station 2, 8 km seaward of the mouth of the Fraser River. The solid line represents the time series on 7–8 August 1991 (▲: sampling times); and the dotted line represents the time series on 23–24 August 1990 (▽: sampling times).

$$\text{Richardson number} = (\boldsymbol{g}/\rho)\ (\mathrm{d}\rho/\mathrm{d}z)/(\mathrm{d}u/\mathrm{d}z)^2$$

where $\boldsymbol{g}$ is gravity acceleration, ρ is density, $\mathrm{d}\rho/\mathrm{d}z$ is the vertical density gradient and $\mathrm{d}u/\mathrm{d}z$ is the velocity shear in the vertical. The u direction is taken to be parallel to the surface flow; the perpendicular component is generally small. Including the perpendicular component in the calculation would make the Richardson numbers slightly smaller, so our calculation is an upper bound for the value. A gradient Richardson number of 0·25 is a critical value below which the velocity shear is strong enough to overcome the density gradient and result in entrainment.

Results and discussion

Figure 1 shows the winds and tides for the two time series at station 2. The winds were much stronger during 7–8 August 1991 than during 23–24 August 1990. The strong

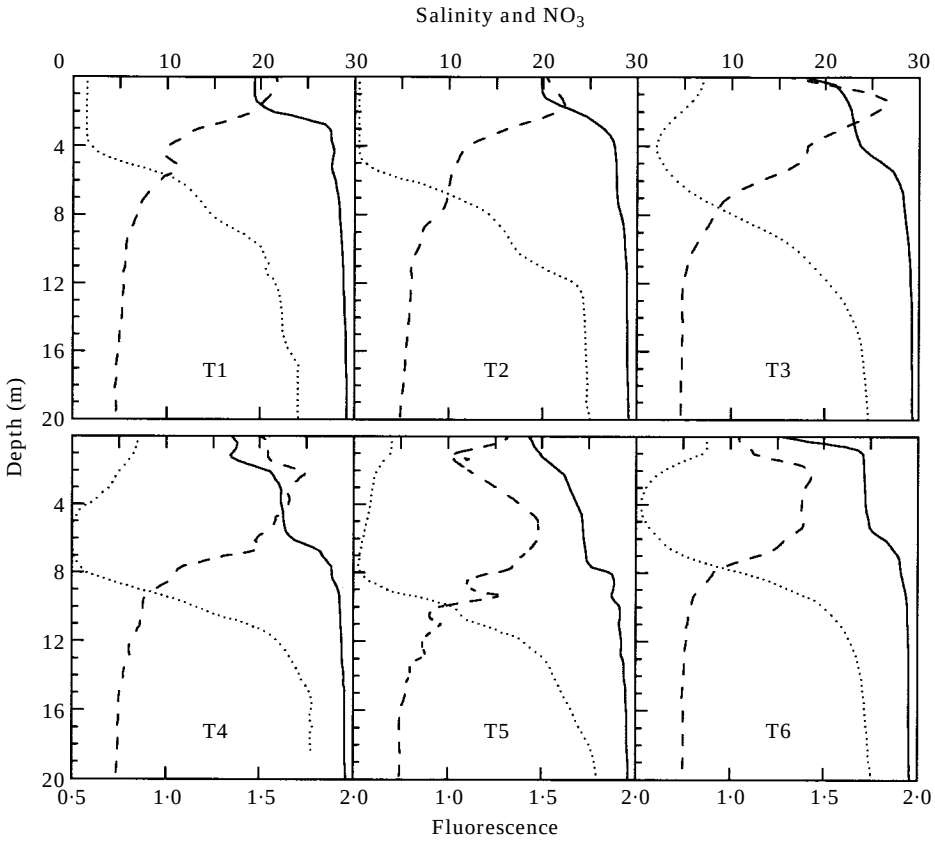

Figure 2. Times series of six vertical profiles of (——) salinity, (· · · ·) NO_3 (μM) and (– – –) fluorescence under weak winds for 23–24 August 1990.

winds on 7–8 August were greatly reduced after the time series. The direction of the stronger winds was persistently from the north. The time series of weak winds on 23–24 August 1990 is presented as a control for the windy time series.

Weak winds

The time series of vertical profiles of salinity, NO_3 and fluorescence for 23–24 August 1990 are shown in Figure 2. At T1 and T2, there was a shallow mixed surface layer (about 2 m). At T3 during the tidal flood, a weak riverine plume was present. When the riverine plume flowed to station 2 in the top 1–2 m at T4, T5 and T6, the mixed layer became deeper (6–8 m) (Figure 2). The T-S diagrams (Figure 3) basically show that there are three water masses and that all the lines (indicating water masses) are smooth. Although the invasion of the riverine plume was observed during T4 to T6 (Figure 3), the estuarine plume size (proportion) appeared to be larger in the upper 10 m during T4 to T6 than during T1 to T3 (Figure 4). Also, during T4 to T6, the deep seawater proportion in the same upper 10 m was reduced (Figure 4). An increase in NO_3 concentration at the surface was accompanied by the invasion of the riverine plume and a NO_3 minimum was located within the middle mixed layer which is dominated by the

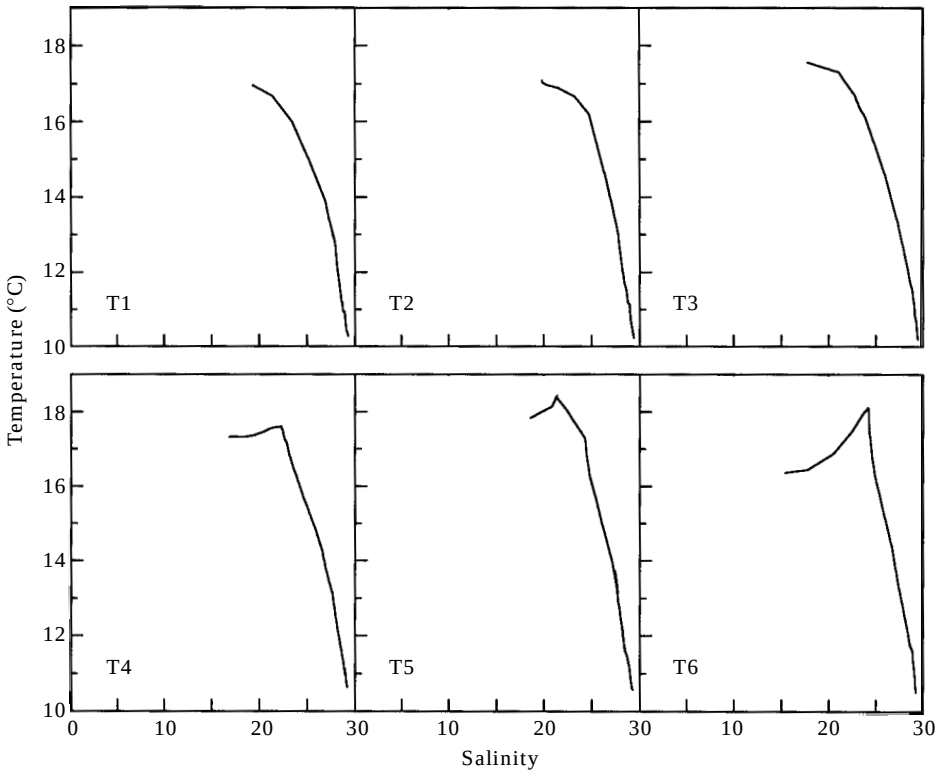

Figure 3. Time series of T-S diagrams under weak winds on 23–24 August 1990.

estuarine plume water (Figure 2). Fluorescence vertical profiles were almost mirror images of the NO_3 distribution, the fluorescence maximum coincided with the NO_3 minimum except at T3 (Figure 2).

Strong winds

Since the wind blew towards the south and the riverine plume usually turns to the north due to the Coriolis force, these forces would tend to balance out and allow the riverine plume to pass station 2. Figure 5 shows the time series of vertical profiles of salinity, NO_3 and fluorescence during the strong wind event on 7–8 August 1991. At T1, 1 h after LLW, the riverine plume was already observed at station 2. During the middle of the flood (T2), the riverine plume became distinct. In the T-S diagram in Figure 6, the T2 curve at salinity <23 representing a mixture of the riverine and estuarine plumes, is not straight as at T1, suggesting entrainment of water that is colder than the water of the estuarine plume. By T3 during the higher high water (HHW), the riverine plume was mixed in the top 2 m. The corresponding T-S diagram reveals that much colder seawater had been entrained (Figure 6). During the rest of the time series, the riverine plume appeared to be present but gradually mixed with other water masses. The water column was basically multi-layered and the halocline became broadened and gradual, indicating the presence of entraining and vertical mixing processes (Figures 5 and 6). The halocline

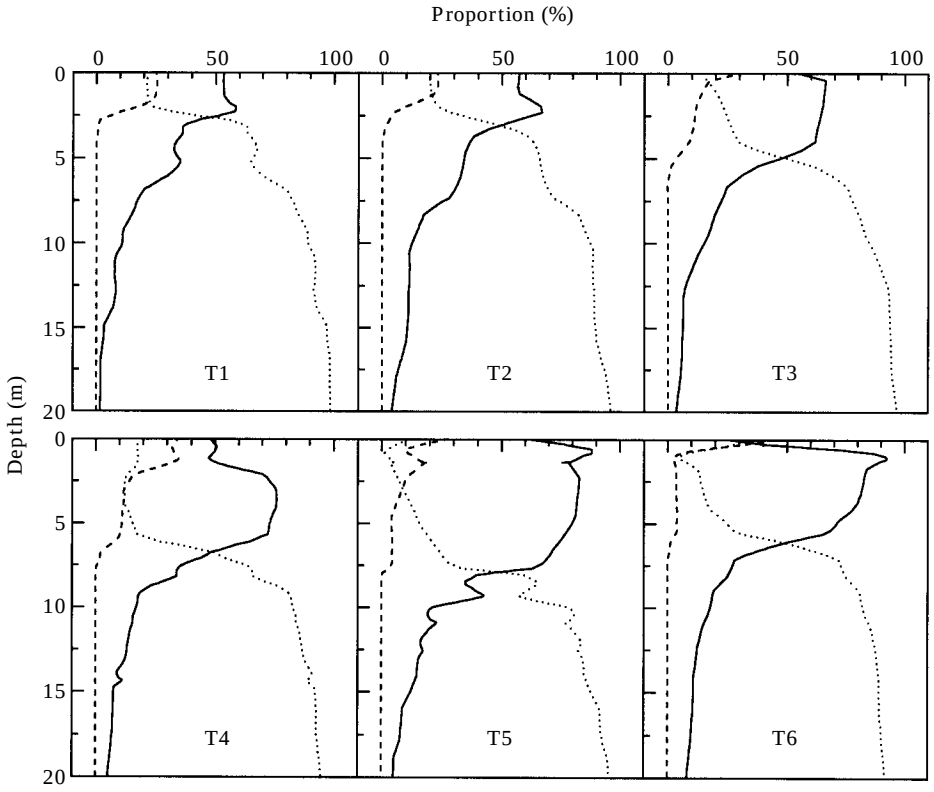

Figure 4. Time series of vertical distribution of the proportion of (– – –) freshwater, (——) estuarine plume and (· · · ·) deep seawater under weak winds on 23–24 August 1990.

extended to the deeper layer below 12 m during T6 to T8, a result of gaining a water volume due to wind-assisted entrainment by the riverine plume. The vertical mixing becomes clearer in the T-S diagrams (Figure 6). During T1 to T4, the riverine plume and the estuarine plume were readily apparent. During T5 to T8, however, they were almost mixed into one line as shown on the T-S diagrams, indicating that the water column became almost one water mass.

The slopes for the T-S line segments to the right of salinity 25 were also a bit lower for T5 to T8 than the ones for T1 to T4 (Figure 6), indicating fresher water penetrating deeper by wind mixing. The tidal stage might also play a role in this mixing process. As the tide approached high water levels at T5, T6 and T7 (Figure 1), the river outflow would slow down and even be dammed. While the wind continued to blow and exert a force on the surface, the remaining riverine plume water was mixed deeper. Although our observation at a fixed station could not separate horizontal advection from vertical mixing, it is reasonable to assume that the water masses advected to station 2 from other areas were subjected to the same wind force. It also should be mentioned that mixing among the three water types into one water mass (one slope in a T-S diagram) does not mean homogeneous mixing since there are still salinity gradients throughout the upper part of the water column (Figure 5).

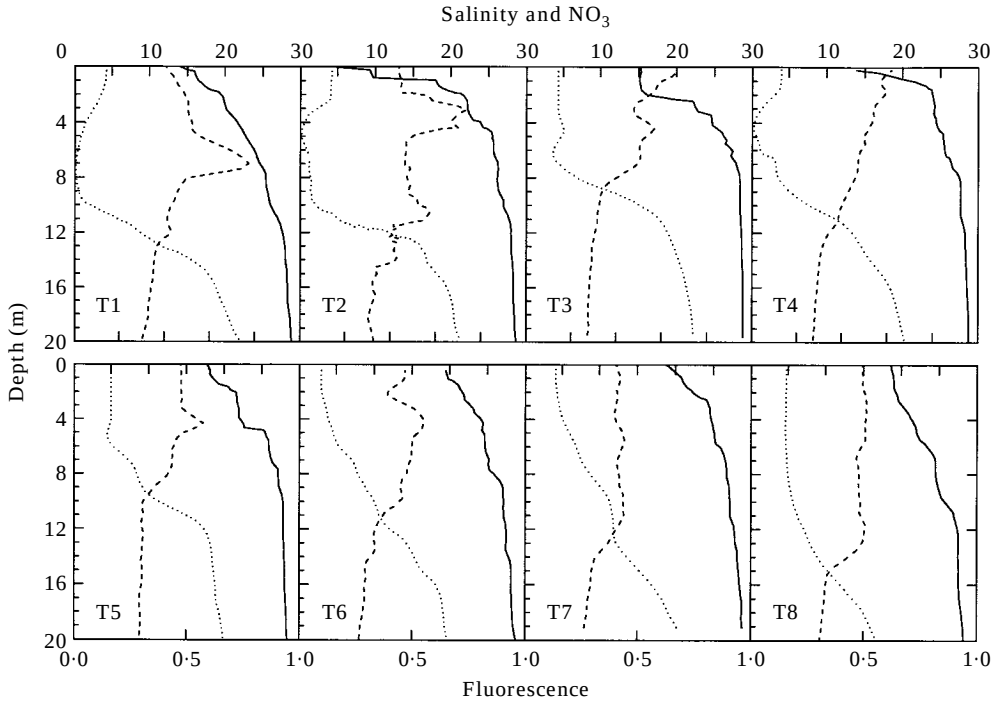

Figure 5. Time series of eight vertical profiles of (——) salinity, (· · ·) NO_3 (μM) and (– – –) fluorescence under windy conditions on 7–8 August 1991.

The vertical NO_3 distribution also demonstrated a clear response to wind mixing (Figure 5). A NO_3 minimum was present during T1 to T5 and disappeared during T6 to T8. The disappearance of the NO_3 minimum in the water column was eventually due to entrainment of NO_3-rich deep seawater into this 4–8 m layer because the riverine plume water mixing with the estuarine plume would reduce NO_3 to levels lower than the river water NO_3 or the initial surface NO_3 of the time series. As shown in Figure 5, the surface NO_3 concentrations remained similar throughout the time series, or were slightly higher at the end. Since the NO_3 minimum occupied a relatively thick layer of the water column, the vertical mixing of the riverine plume, the estuarine plume and the deep seawater resulted in a decrease in NO_3 concentrations in the lower layer during T6 to T8, compared to earlier times.

Fluorescence responded to wind mixing and its change reflected closely the change in NO_3 distribution (Figure 5). The fluorescence maximum coincided with the NO_3 minimum initially and then it became mixed in the upper layer when the NO_3 minimum was eroded. Note that phytoplankton cells did not appear to be lost during mixing from the upper stratified layer, as shown by the distribution of fluorescence (Figure 5). These phytoplankton cells could rapidly respond to the increase in nutrients.

The change in the distribution of salinity, NO_3 and fluorescence during the time series indicated vertical mixing among the three water types. Figure 7 shows vertical profiles of velocity and Richardson numbers as well as salinity. Currents were strong at the surface and were reduced in the lower layer. Most of the time, there was two-layer flow in the water column (T2, T3, T5, T6 and T7). The surface layer flowed in one

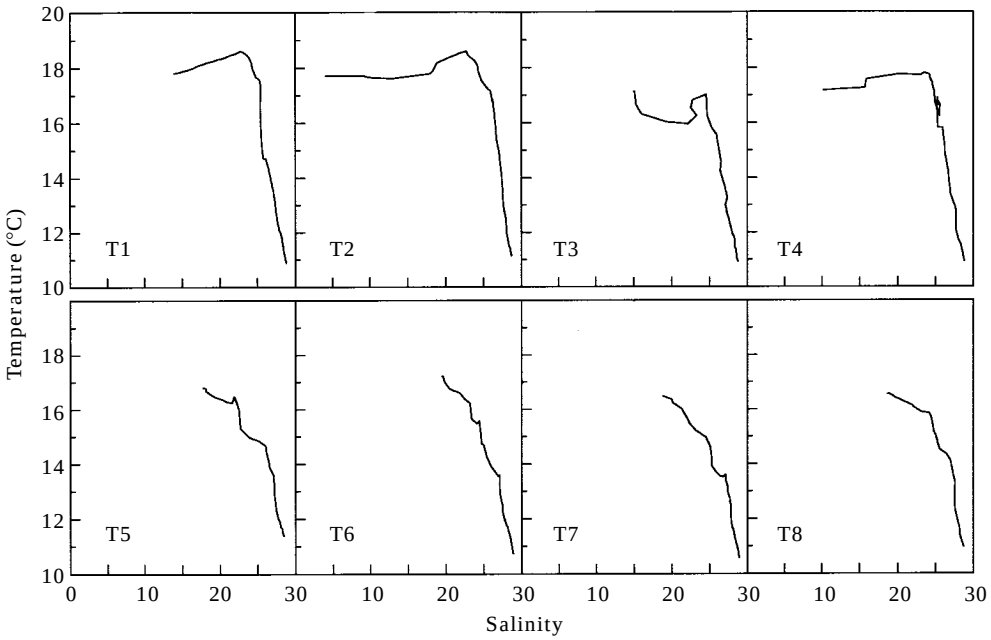

Figure 6. Time series of T-S diagrams under windy conditions on 7–8 August 1991.

direction and the water below flowed in the opposite direction. There was a depth at which the two flows moved opposite to each other and hence the current speed was zero. This depth will be referred to as the null depth. A halocline was also located at the null depth. A strong shear often occurred near the null depth because of the two flows moving opposite each other. Mixing most likely took place near this depth. Richardson numbers (Figure 7) indicated that parts of the water column were very turbulent because Richardson numbers were often less than 0·25. A Richardson number of 0·25 is a critical value below which a shear velocity is considered to be strong enough to overcome a density stability and allow turbulence and turbulent mixing to occur (Partch & Smith, 1978; Dyer & News, 1986; Geyer & Farmer, 1989). As shown in Figure 7, Richardson numbers less than 0·25 frequently occurred near the null depth. As entrainment and mixing took place, the upper layer became thicker. Another indication of entrainment was that the null zone moved noticeably deeper near the end of the time series (T5, T6 and T7). The water of the surface layer was also getting heavier as the denser deep seawater was entrained upward and mixed as the wind continued blowing. This deepening slowed down the surface layer flow near the end of the time series even before the wind speeds were reduced. Interestingly, the rapid changes in velocities and salinities frequently coincided with each other (Figure 7), indicating a close coupling between the water flows and salinity structure. Particularly, the null depth was sometimes located right at a major halocline (T2, T3 and T5; Figure 7).

The result of wind-induced entrainment and mixing is clearly shown in Figure 8; over the time series, freshwater penetrated deeper, the estuarine plume volume shrunk in the top 10 m and the deep seawater proportion increased in the same layer and at the surface as well.

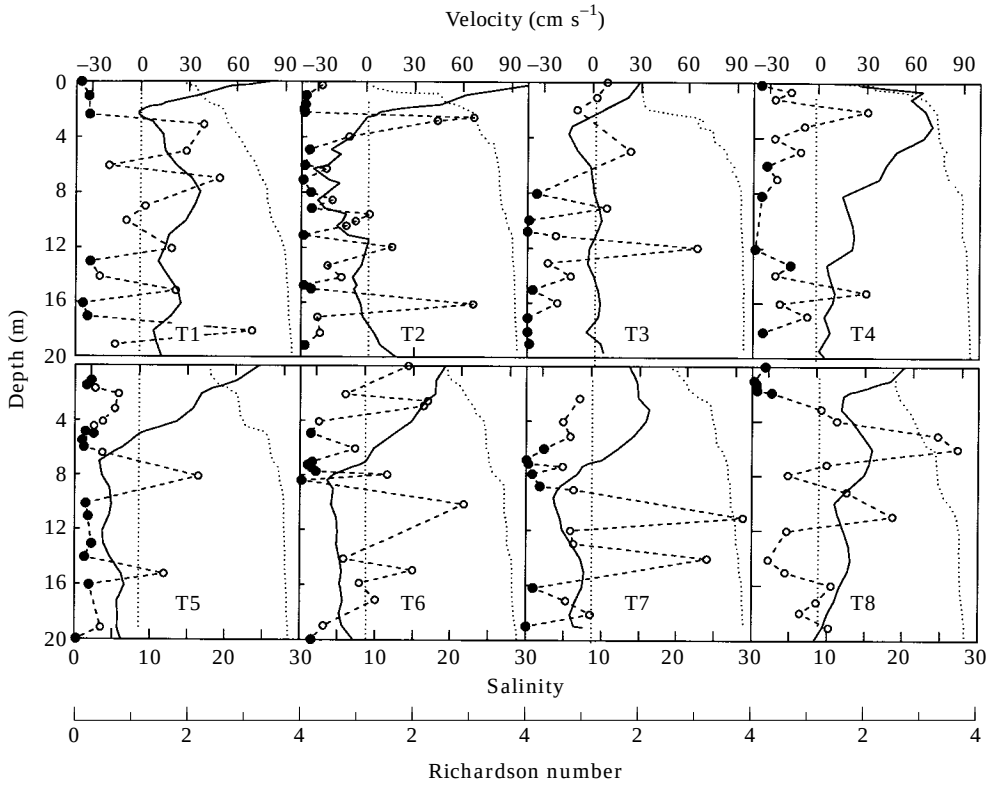

Figure 7. Time series of vertical profiles of velocity (——) and Richardson numbers (circles) under windy conditions on 7–8 August 1991. The velocity shown is the component in the direction of the surface flow, which changes somewhat between the vertical profiles. The component perpendicular to the surface component is generally small. The vertical dotted line delineates zero in velocity. The filled circles indicate Richardson numbers that are <0·25. Salinity (· · · ·) is also plotted for comparison.

Strong vs. *weak winds*

The equivalent thickness of entrained seawater was thicker during the strong wind time series [Figure 9(b)] than during the weak wind time series [Figure 9(a)]. Also shown in Figure 9(b) are tidal effects. Entrainment of the deep seawater and the freshwater penetration depth (bottom depth of the sum of the three equivalent thicknesses) appeared to decrease during the flood (T2) and high waters (T3 and T4), and then to increase (T5, T6 and T8).

Entrainment of the deep seawater affected entrainment of NO_3. A regression analysis (data not shown) indicated that 97% of the amount of entrained NO_3 was accounted for by the equivalent thickness of the entrained deep seawater during the strong wind event and 72% during the weak wind time series. Regression analyses (data not shown) also indicated that depth-integrated fluorescence was explained by the volume (equivalent thickness) of the estuarine plume during both time series (R^2>0·9). The amount of entrained NO_3 under strong wind conditions was increased compared to weak wind conditions, as shown in Table 1 which summarizes a comparison between the two time series. The ratio of the entrained deep seawater to freshwater during the windy time

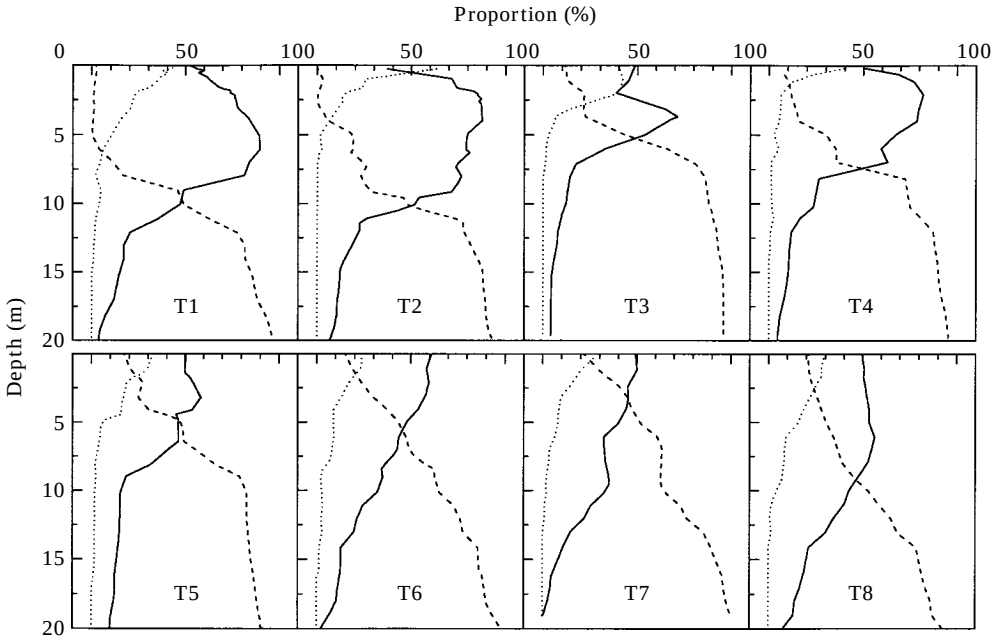

Figure 8. Time series of vertical distributions in the proportion of (· · · ·) freshwater, (——) the estuarine plume and (– – –) the deep seawater under windy conditions on 7–8 August 1991.

series was highest among all the time series (Yin *et al.*, 1995*b*; present study). A possible explanation is that for the same amount of freshwater released from the river, speeds of the riverine plume must have increased when constant winds blew in the right direction. In other words, the momentum and kinetic energy of the riverine plume was increased by winds. Therefore, more deep seawater was mixed with freshwater. At the same time, freshwater penetrated deeper (3 m deeper for the windy condition than for weak winds in Table 1). The contribution of entrained NO_3 was 12 times the river-borne NO_3 for the strong wind event and 5·6 times for the weak wind time series. Although low NO_3 concentrations in the river (<4 μM) are mainly responsible for these high ratios, the high contribution of entrained NO_3 indicates that entrainment of NO_3 in summer is particularly important in supplying NO_3 and supporting new primary production for the region when NO_3 concentrations are low in the river.

During the time series of 23–24 August 1990, the tidal conditions were close to a neap tide and river discharge was lower, whereas the time series of 7–8 August 1991 was conducted during a pre-spring tide and under higher river discharge. Certainly, as shown in the previous study (Yin *et al.*, 1995*b*), a higher tidal range and river discharge contributed to entrainment of NO_3 during the strong wind event. However, the amount of entrained NO_3 (44 mmol m^{-2}) during the wind event of 7–8 August 1991 was even more than the amount (32 mmol m^{-2}) during the time series of 29–30 May 1990, which was conducted during a higher tidal range and higher river discharge but low winds (3·6 m s^{-1}) (see Table 2 in Yin *et al.*, 1995*b*). The winds were mainly responsible for the higher entrainment of NO_3 during the 7–8 August time series. Other strong evidence for the wind effect is that the NO_3 minimum layer was broken down by winds.

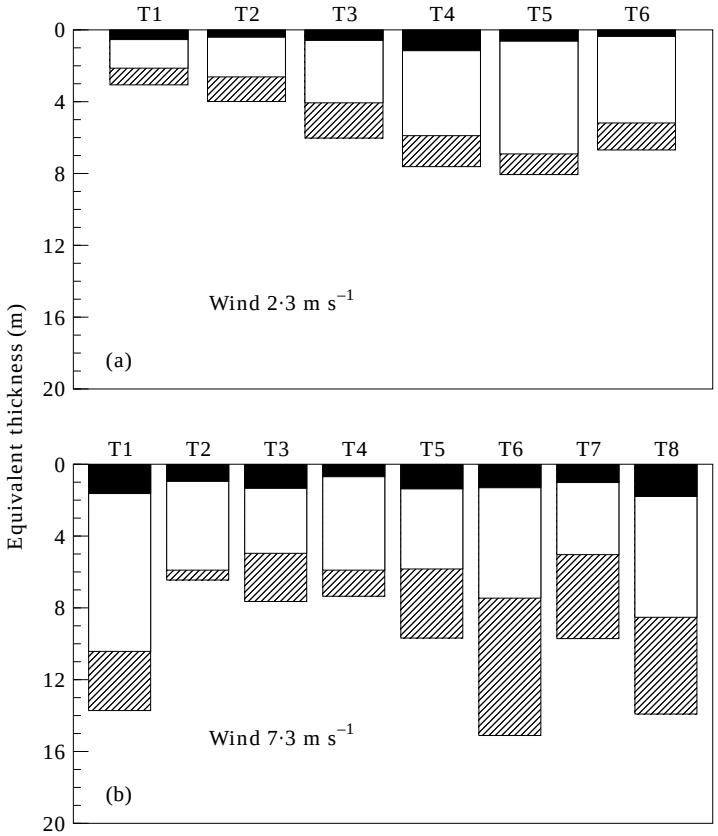

Figure 9. Time series of the equivalent thickness of freshwater (■), the entrained estuarine plume (□) and the entrained deep seawater (▨) under (a) a weak wind condition on 23–24 August 1990 and (b) a strong wind condition on 7–8 August 1991.

This wind effect is comparable with the time series near the maximum river discharge which swept the NO_3 minimum away (Yin *et al.*, 1995*b*).

When the water column is more stratified, more energy will be required to break down stratification. If a pycnocline is strong, the surface flow can be decoupled from the water below (Buckley & Pond, 1976). Therefore, the degree of vertical mixing in the water column depends on stratification and the depth of stratification. The degree will increase with the distance away from the river mouth since the riverine plume produces a greater salinity gradient close to the river mouth. The increase in vertical mixing with distance was shown in the vertical profiles along a transect of stations from station 2 to 110 km north in the Strait of Georgia (Yin *et al.*, unpubl. data). Those vertical profiles were conducted on the same day after the end of the time series on 8 August 1991. The water column further seaward was more mixed and NO_3 concentrations were increased in the surface layer compared to the profile at T8 in Figure 5. A recent model for the same region also suggests that the water column will be more mixed by a constant wind speed at an area further away than for an area near the river mouth (St John *et al.*, 1993).

Phytoplankton cells during the wind event remained in the surface mixed layer (which was still stratified within itself and relative to the layer below), as shown in vertical

TABLE 1. Comparisons between the weak wind condition on 23–24 August 1990 and the strong wind condition on 7–8 August 1991. All the parameters are time-averaged over the time series

Parameter	Weak winds	Strong winds
Sampling period (h)	20·5	21·7
Tidal range (m)	2·6	3·8
Mean tidal height (m)	3·0	3·1
Wind speed ($m\ s^{-1}$)	2·3[a]	7·3[b]
Discharge ($m^3\ s^{-1}$)	2890	4200
Equivalent thickness (m)		
Freshwater	0·7	1·1
Entrained estuarine plume (EEP)	4·1	4·9
Entrained deep seawater (EDW)	1·5	3·5
Freshwater-penetration depth (m)	6·4	9·5
Entrained NO_3 ($mmol\ m^{-2}$)	15·9	43·7
River-borne NO_3 ($mmol\ m^{-2}$)	2·8	3·7
Depth-integrated fluorescence (m^{-2})	7·7	3·1
Ratio of sum of EEP and EDW to freshwater	8·0	8·8
Ratio of EDW to freshwater	2·1	3·0
Ratio of entrained NO_3 to river-borne NO_3	5·6	12·0

[a] There was no dominant wind direction.
[b] Winds from the north were dominant.

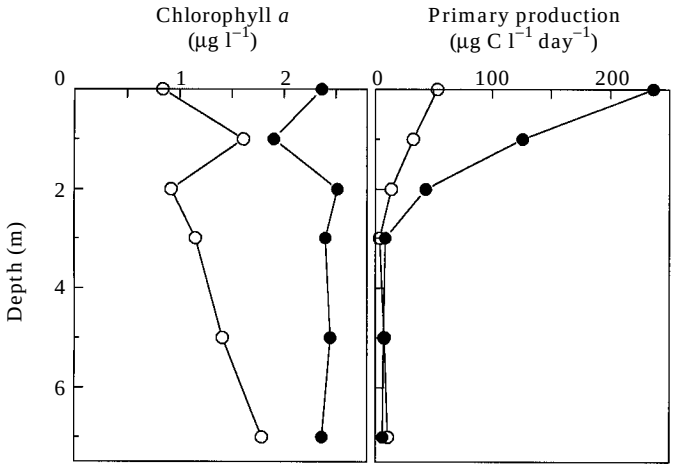

Figure 10. Vertical profiles of chlorophyll *a* and primary production at the beginning (T1) and the end (T8) of time series on 7–8 August 1991. ○, 7 August, 10.00h; ●, 8 August, 07.45h.

profiles of fluorescence in Figure 5. They should be capable of taking up the entrained nutrients quickly and growing rapidly. In Figure 10, vertical profiles of chlorophyll and primary production at the beginning and end of the windy time series show that both chlorophyll and primary production were increased at the end (T8) compared to the beginning (T1). The difference in primary production between the profiles was not due to differences in surface irradiance since daily solar radiation on 8 August was even lower on 7 August. In fact, a summer wind-induced bloom was observed in the estuarine

plume immediately after this wind event (Yin *et al.*, unpubl. data). Such a rapid response is different from wind effects producing upwelling in coastal oceans, where it usually takes days to weeks for upwelled phytoplankton to respond to the upwelled nutrients and improved light conditions (MacIsaac *et al.*, 1985; Zimmerman *et al.*, 1987).

In conclusion, under windy conditions, entrainment of NO_3 was increased compared to weak winds. High winds enhanced the effects of tidal conditions and the magnitude of river discharge. Winds transferred horizontal momentum to the surface layer and induced a strong shear between the different layers, which could be sufficient for across-pycnocline mixing. As a result of wind-induced entrainment, phytoplankton cells remained in the euphotic zone and could take up the entrained nutrients rapidly, enabling the development of a summer phytoplankton bloom.

Acknowledgements

We thank Dr Mike St John and Peter Clifford who coordinated the cruises and the following cruise participants: Robert Goldblatt and Heidi Saywer. David Jones helped to set up the vertical profiling system. Thanks are given to the Department of Fisheries and Oceans for providing ship time, and the officers and crew of C.S.S. *Vector* for their assistance. The comments by Drs James Cloern, Ken Denman and Peter Franks improved the manuscript.

This research was funded by a Natural Sciences and Engineering Research Council of Canada (NSERC) Strategic grant. The Research Fellowship to support K. Yin was kindly provided by the Department of Fisheries and Oceans, Pacific Biological Station, Nanaimo, British Columbia, Canada.

References

Buckley, J. R. & Pond, S. 1976 Wind and surface circulation of a fjord. *Journal of the Fisheries Research Board of Canada* **33,** 2265–2271.

Denman, K. L. & Powell, T. M. 1984 Effects of physical processes on planktonic ecosystems in the coastal ocean. *Oceanography and Marine Biology: Annual Review* **22,** 125–168.

Dyer, K. R. & News, A. L. 1986 Intermittency in estuarine mixing. In *Estuarine Variability* (Wolf, D., ed.). Academic Press, New York, pp. 321–339.

Farmer, D. M. 1972 The influence of the wind on the surface waters of Alberni Inlet, Ph.D. Thesis, University of British Columbia, Vancouver, 92 pp.

Foster, P., Beardall, J., Voltolina, D. & Savidge, G. 1985 The effects of wind, phytoplankton and density discontinuities upon ammonia distribution in Liverpool Bay. *Estuarine, Coastal and Shelf Science* **20,** 463–475.

Geyer, W. R. & Farmer, D. M. 1989 Tide-induced variation of the dynamics of a salt wedge estuary. *Journal of Physical Oceanography* **19,** 1060–1072.

Jones, D. M., Harrison, P. J., Clifford, P. J., Yin, K. & St John M. A. 1991 A computer-based system for the acquisition and display of continuous vertical profiles of temperature, salinity, fluorescence and nutrients. *Water Research* **25,** 1545–1548.

LeBlond, P. H. 1983 The Strait of Georgia: functional anatomy of a coastal sea. *Canadian Journal of Fisheries and Aquatic Science* **40,** 1033–1063.

MacIsaac, J. J., Dugdale, R. C., Barber, R. T., Blasco, D. & Packard, T. T. 1985 Primary production cycle in an upwelling center. *Deep-Sea Research* **32,** 503–530.

Mann, K. H. & Lazier, J. R. N. 1991 *Dynamics of Marine Ecosystems; Biological–Physical Interactions in the Oceans*. Blackwell Scientific Publications, Oxford, 466 pp.

Partch, E. N. & Smith, J. D. 1978 Time dependent mixing in a salt wedge estuary. *Estuarine and Coastal Marine Science* **6,** 3–19.

Royer, L. & Emery, W. J. 1982 Variations of the Fraser River plume and their relationship to forcing by tide, wind and discharge. *Atmosphere-Ocean* **20,** 357–372.

St John, M. A., Marinone, S. G., Stronach, J., Harrison, P. J., Fyfe, J. & Beamish, R. J. 1993 A horizontal resolving physical–biological model of nitrate fluxes and primary productivity in the Strait of Georgia. *Canadian Journal of Fisheries and Aquatic Science* **50,** 1456–1466.

Yin, K., Harrison, P. J., Pond, S. & Beamish, R. J. 1995*a* Entrainment of nitrate in the Fraser River estuary and its biological implications. I. Effects of the salt wedge. *Estuarine, Coastal and Shelf Science* **40,** 505–528.

Yin, K., Harrison, P. J., Pond, S. & Beamish, R. J. 1995*b* Entrainment of nitrate in the Fraser River estuary and its biological implications. II. Effects of spring *vs*. neap tides and river discharge. *Estuarine, Coastal and Shelf Science* **40,** 529–544.

Zimmerman, R. C., Kremer, J. N. & Dugdale, R. C. 1987 Acceleration of nutrient uptake by phytoplankton in a coastal upwelling ecosystem: a modeling analysis. *Limnology and Oceanography* **32,** 359–367.